

JET-SUSPENDED, CALCITE-BALLASTED CYANOBACTERIAL WATERWARTS IN A DESERT SPRING¹

Ferran Garcia-Pichel,² Bman D. Wade

Department of Microbiology, Arizona State University, Tempe, Arizona 85287, USA

and

Jack D. Farmer

Department of Geological Sciences, Arizona State University, Tempe, Arizona 85287, USA

We describe a population of colonial cyanobacteria (waterwarts) that develops as the dominant primary producer in a bottom-fed, O₂-poor, warm spring in the Cuatro Ciénegas karstic region of the Mexican Chihuahuan Desert. The centimeter-sized waterwarts were suspended within a central, conically shaped, 6-m deep well by upwelling waters. Waterwarts were built by an *Aphanothece*-like unicellular cyanobacterium and supported a community of epiphytic filamentous cyanobacteria and diatoms but were free of heterotrophic bacteria inside. Sequence analysis of 16S rRNA genes revealed that this cyanobacterium is only distantly related to several strains of other unicellular cyanobacteria (*Merismopedia*, *Cyanothece*, *Microcystis*). Waterwarts contained orderly arrangements of mineral crystallites, made up of microcrystalline low-magnesium calcite with high levels of strontium and sulfur. Waterwarts were 95.9% (v/v) glycan, 2.8% cells, and 1.3% mineral grains and had a buoyant density of 1.034 kg·L⁻¹. An analysis of the hydrological properties of the spring well and the waterwarts demonstrated that both large colony size and the presence of controlled amounts of mineral ballast are required to prevent the population from being washed out of the well. The unique hydrological characteristics of the spring have likely selected for both traits. The mechanisms by which controlled nucleation of extracellular calcite is achieved remain to be explored.

Key index words: buoyancy; calcite precipitation; colony formation; cyanobacteria; deserts; warm springs

Abbreviations: BLAST, basic local alignment search tool; DAPI, 4,6-diamidino-2-phenylindole; DGGE, denaturing gradient gel electrophoresis; ICDD, International Center for Diffraction Data

The Cuatro Ciénegas Basin (Coahuila, Mexico) is a complex karstic system in which the underlying Cretaceous limestone, dolomite, and gypsum formations are actively dissolved by an aquifer of distant origin. This results in the formation of innumerable springs, surface and underwater streams, caves, and sinkholes

(“pozas”) which are famous for their beauty and the biological diversity they harbor (Grall 1995). Cyanobacteria are often dominant primary producers in calcareous freshwater springs (Pentecost and Whitton 2000). In most cases they are sessile, benthic, or epiphytic and are also typically associated with the precipitation of microcrystalline calcite (algal micrite), which in some cases results in the formation of macroscopic stromatolitic structures (“living” stromatolites). The algal flora in the Cuatro Ciénegas Basin fresh waters is no exception, particularly with regard to the widespread formation of laminated calcified microalgal communities (Winsborough and Golubic 1987, Winsborough et al. 1994).

During a survey of Cuatro Ciénegas cyanobacterial communities, we noted Escobedo’s warm spring, a sheltered, small, fast flowing spring where planktonic populations of marble-sized colonies of blue-green algae developed. Although buoyant planktonic cyanobacterial populations are known from hard-water lakes (Konopka 1989) and small karstic sinkholes (Camacho et al. 1996), the nature of the spring itself made the presence of large-sized cyanobacterial assemblages an apparent paradox. First, planktonic populations do not usually develop in swift streams and spring-fed small lakes in the area. Second, planktonic populations of large colonial cyanobacteria, such as *Trichodesmium*, *Aphanizomenon*, or *Nodularia*, are positively buoyant by virtue of their intracellular gas vesicles (Walsby 1994) and develop in open waters where wind-forcing circulates them in the mixed layer. Under wind-sheltered conditions, such as those reigning in Escobedo’s spring, positively buoyant cyanobacteria should float to the surface and subsequently be washed out.

Most cyanobacteria-dominated communities found in waters of the Cuatro Ciénegas Basin undergo extensive calcification. This is also the case along the shore ledges of Escobedo’s spring, where calcifying cyanobacteria and diatoms form stromatolitic mats. However, such calcification would force the waterwarts to sink to the spring’s bottom. Here we present a study addressing various aspects of this most unusual cyanobacterial habitat.

MATERIALS AND METHODS

Field observations and sampling Escobedo’s warm spring (N 26° 54′ 229, W 102° 04′ 590) surfaces through a large (ca. 1-km

¹ Received 26 September 2001. Accepted 14 February 2002.

² Author for correspondence: e-mail ferran@asu.edu.

wide) travertine mound that is a relic of a long history of carbonate spring deposition. It has long been used as a local recreational area. We visited the spring during December 2000, carrying out observations and taking samples of the biota, and in April 2001, conducting morphometric, chemical, and biological measurements and sampling. A bathymetric map (Fig. 1) of the present spring was done by triangulation from the shore and manual depth sounding. Flow measurements were conducted at the western inlet and the main outlet by spatial integration of point measurements of flow velocity taken on a cross-sectional plane, ca. 30 cm apart. Water velocity was measured with an FP101 flow probe (Global Water Instrumentation, Inc., Gold River, CA, USA). Dissolved oxygen and temperature profiles were measured with a YSI oxygen meter (Yellow Springs Instruments, Yellow Springs, OH, USA) attached to a submersible sensor. Light intensity (downwelling irradiance) depth profiles were measured with a LiCor meter (LiCor, Lincoln, NE, USA) attached to a submersible cosine-corrected PAR sensor (LiCor). Samples of waterwarts were collected by diving, using a small fish net. Samples for molecular analyses were placed in sterile microcentrifuge tubes, immediately frozen in liquid N_2 on site, transported, and kept frozen (-80°C or lower) until DNA isolation. Samples for volumetric, gravimetric, and mineralogical analyses were stored in local water in a plastic container and transported to the laboratory for analyses. Samples for morphometric analyses were immediately fixed with 3% formaldehyde. Unfixed samples remained apparently unchanged for several months if kept at room temperature under gentle shaking and moderate light intensities ($50\text{--}100\ \mu\text{mol photons}\cdot\text{m}^{-2}\cdot\text{s}^{-1}$, PAR). Storage at 4°C caused apparent disintegration of the cellular fraction within 3–4 weeks.

Morphometric and gravimetric measurements. For size distribution determination, 100 waterwarts were randomly selected, deposited on a Petri dish containing 1% solidified agar, and their maximum diameter measured to the nearest millimeter with a ruler. For the determination of buoyant density, five groups of waterwarts were collected, strained, blotted on paper towels, and weighed to yield around 30–50 g each. They were resuspended in 50 mL of distilled water in a volumetric cylinder, and the new volume was recorded. Waterwart volume was obtained by subtraction. Buoyant densities were calculated from the

weight-to-volume ratios. The groups were pooled and dried at 70°C overnight to obtain a measure of dry weight and then ashed at 650°C for 6 h to obtain the ash content.

Sectioning, staining, and microscopy. Individual waterwarts were embedded in a liquid, 50°C , 1.5% aqueous agar solution. After agar solidification, thick sections (1 mm) were cut from agar blocks containing waterwarts using a tabletop microtome. Sections were placed on agar Petri dishes to prevent desiccation and observed within 1–3 h. Some sections were stained with 4,6-diamidino-2-phenylindole (DAPI, Sigma) by immersion in a $10\text{ mg}\cdot\text{L}^{-1}$ solution for 25 min and washed for 3 min in distilled water. Cyanobacterial cells were adequately stained, demonstrating complete penetration of DAPI into the sections. For overall morphology, sections were photographed under a Nikon SMZ-U dissecting photomicroscope (Nikon, Tokyo, Japan) with basal illumination. For determination of the distribution of heterotrophic bacteria, DAPI-stained sections were observed and photographed under oil immersion with a Nikon Eclipse E800 dual-interference contrast/fluorescence photomicroscope (Nikon) under UV excitation (excitation, 340–380 nm; emission, 435–485 nm). Blue excitation (excitation, 450–490; emission >520) was used to detect chl *a* and phycobilin red autofluorescence. Initial mineralogical analyses were carried out using a Nikon Eclipse E600 polarizing photomicroscope (Nikon) under bright-field (plane-polarized) and crossed-polarized illumination.

Volume partitioning of waterwarts. Waterwarts were collected, strained, blotted, and their volume measured as explained above. The suspension was blended to uniformity twice for 1 min in a Waring blender and dispensed into 50-mL conical-end plastic centrifuge tubes (Dyna-mic Corp, New Hartford, CT, USA). Tubes were centrifuged for 40 min at $2500g$ and the clear supernatant decanted. Fifty milliliters of distilled water was added, and the mixture blended, centrifuged, and decanted again. Pellets were collected and resuspended in 200 mL of distilled water to which 0.5 mL of a 2% detergent solution (RBS pF, VWR Scientific Products, Brisbane, CA, USA) was added. The mixture was blended again 10 times for 15 s each, allowing 1–2 min in between for the foam to settle. After two additional hour-long settling times at 4°C , remaining foam was removed. At this point, cells, minerals, and extracellular glycan could be separated by differential centrifugation ($2000g$, 20 min). The

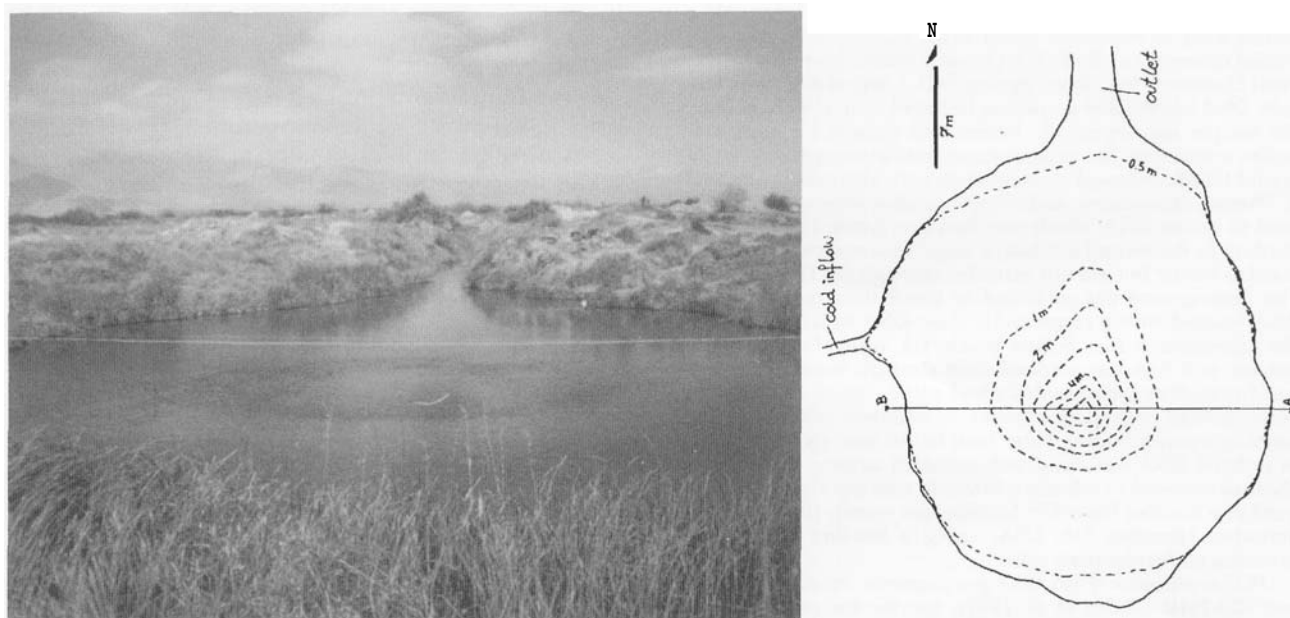


FIG. 1. Escobedo's warm spring: general view (left) and bathymetric map (right). A sampling and reference line above the spring transecting the central well can be seen in the photograph, which is drawn (AB) in the map for reference.

supernatants were clear, indicating that no loss of phycobilins had taken place, and thus cell integrity was ensured. Microscopic inspection of the cellular fraction revealed intact cells after this procedure. For purification, the last centrifugation step was repeated three times, with gentle mixing, each time decanting the polysaccharide-rich supernatant and substituting it with distilled water. The cell fraction and mineral phase were separated by careful pipetting and collected in custom-graduated 1.5-mL microcentrifuge tubes, which were used to determine the packed volume of each fraction. After several washes with distilled water, the mineral fraction was used for mineralogical analyses.

X-ray diffraction and electron microprobe analyses. Confirmation of mineralogy was done using x-ray powder diffraction in combination with electron microprobe analysis of polished thin sections. Fine-grained mineral separates were obtained from colonies by centrifuging (see above). Grains were suspended in 100% ethanol and then dispersed onto a sample holder ("zero background" thin quartz plate) to form a thin layer covering an area about 1 cm². X-ray diffraction analysis was carried out using a Siemens automated x-ray diffractometer fitted with a Cu-anode x-ray tube (Cu K α = 1.5406 Å). The instrument was operated in a summation step-scan mode at 40 kV (30 mA), and data were obtained over a 2-theta range of 5–90 degrees using a 7-degree detector. Mineralogical identifications were made using an on-line powder diffraction database provided by the International Center for Diffraction Data (ICDD, www.icdd.com). Elemental analyses of mineral separates were accrued out on a Jeol JXA-8600 electron probe microanalyzer (JEOL USA, Peabody, MA, USA) on polished thin sections of mineral grain mounts.

Microalgal community composition. To determine the composition of eukaryotic and cyanobacterial microalgae forming or inhabiting the waterwort community, we used microscopy, cultivation, and fingerprinting analyses of 16S rRNA genes. Enrichment cultures were set up on both agar-solidified and liquid BG11 minimal medium. Whole waterworts, pieces, and slurries thereof were used as inoculum and incubated at room temperature at light intensities between 50 and 100 $\mu\text{mol photons}\cdot\text{m}^{-2}\cdot\text{s}^{-1}$. Thin sections (as above) and slurries were used for microscopy. Molecular methods are detailed in the following sections.

DNA isolation. Two methods, designed for samples rich in mucopolysaccharides, were used to isolate DNA from waterworts. In the first method, a single waterwort was homogenized in 1 mL of extraction buffer (see below) using a Tenbroeck tissue grinder (VWR International, West Chester, PA, USA). After adding 5 mL of extraction buffer to the homogenate, it was extruded through a chilled (4°C) French press (American Instrument Company, Inc., Silver Spring, MD, USA) at 800 psi to lyse cells. DNA was isolated according to Nübel et al. (1997). Briefly, the sample was repeatedly frozen and thawed in extraction buffer containing the mucopolysaccharide-precipitating compound CTAB, followed by incubation with SDS and proteinase K. Phenol, chloroform, and isoamyl alcohol were subsequently used to isolate DNA, which was then precipitated in isopropyl alcohol. In the second method, a single waterwort was homogenized as before but was not extruded through the French press. The homogenate was subjected to freeze-thaw cycles and its DNA isolated with a commercial plant DNA isolation kit (Mo Bio Laboratories, Inc., Solana Beach, CA, USA). For cultivated isolates, cell lysis was accomplished through homogenization and freeze-thaw cycles as described above, but in 10 mM Tris buffer instead of extraction buffer. In addition, cells were incubated in a gently boiling water bath for 10 min. Quantification of isolated DNA was done with standard agarose gel electrophoresis followed by ethidium bromide staining. Gels were analyzed in a Bio-Rad Fluor-S™ MultiImager system (Bio-Rad Laboratories, Hercules, CA, USA) using a Bio-Rad EZ Load™ precision molecular mass ruler.

PCR amplification of 16S rRNA gene fragments. Primers CYA106F and CYA781R (Nübel et al. 1997), specific for cyanobacteria and plastids, were used for amplification of ca. 600 base pair long 16S rRNA gene fragments in a Bio-Rad iCycler™ thermal cycler. Each 100- μL PCR reaction contained the following: 10

μL of 10 \times Takara Ex Taq™ PCR buffer (PanVera Corporation, Madison, WI, USA), 8 μL of Takara dNTP mixture (2.5 mM each), 50 pmol of each primer, 200 μg of BSA, 20 μL of 5 \times Eppendorf TaqMaster™ PCR-enhancer (Brinkmann Instruments, Inc., Westbury, NY, USA), and 15 ng of isolated DNA. After an initial denaturation at 94°C for 5 min (hot start), 2.5 units of Takara Ex Taq™ DNA polymerase was added to the reaction at 80°C. Thirty-five cycles of 1 min each at 94°C (denaturation), 60°C (annealing), and 72°C (extension) were performed and the reaction finished with a final extension at 72°C for 9 min. Quantification of PCR product was done as above for isolated DNA.

Denaturing gradient gel electrophoresis (DGGE), sequencing, and phylogenetic assignments. DGGE was used to separate and characterize 16S rRNA gene fragments. DGGE uses a gradient of chemical denaturants (urea and formamide) in a polyacrylamide gel to separate DNA fragments of equal length but different melting behaviors (i.e. sequence). Four hundred nanograms of PCR product was electrophoresed through a 20%–60% denaturing gradient according to Nübel et al. (1997) for 4 h at 200 V in a Bio-Rad DCode™ universal mutation detection system and analyzed as described above for agarose gels. For DGGE band sequencing, each band was excised using a sterile scalpel and DNA allowed to diffuse out for at least 3 days at 4°C in 50 μL of 10 mM Tris buffer. One microliter of the solution was PCR amplified using the same primers, reaction mixture, thermocycling conditions, and product quantification as above. A kit was used to purify PCR product (Qiagen, Inc., Valencia, CA, USA), and 150 ng was commercially sequenced in two separate reactions (5' to 3' and 3' to 5'). Complementary sequences were matched, aligned, and edited using Sequence Navigator (Applied Biosystems, Foster City, CA, USA) and submitted to the Basic Local Alignment Search Tool (BLAST, National Center for Biotechnology Information, www.ncbi.nlm.nih.gov) for phylogenetic matching. Sequences obtained from DGGE bands a–f have been deposited in GenBank with accession numbers AY100324–AY100329, respectively.

RESULTS

Spring morphometry, circulation, and physical-chemical characteristics. Most of the spring basin is shallow (<1 m deep, Fig. 1). A central, 6-m deep, conical well, dug several decades ago by the townspeople, contains two thirds of Escobedo's water volume, which amounts to 440 m³. The bottom sediment is soft carbonate sand. Surface water and groundwater feed the spring. A small stream, originating in a nearby springhead, provides 0.063 m³·s^{−1} of well-oxygenated, relatively cold water through an inlet situated at the western shore. Water temperatures at this inlet are variable and close to ambient air temperature. Most of the water, however, jets into the spring from several cavernous openings through the travertine at the bottom of the central well. Water exits the spring through a single outlet channel at the NNE shore. The total discharge measured through the outlet was 0.658 m³·s^{−1}. Mass balance then requires that the deep source account for at least 90% of water inputs. According to the above values, the average residence time of water in the spring is 669 s (11.1 min). The water from the deep source is warm (34.8°C) and severely depleted in dissolved oxygen (around 4% air saturation) but does not bear appreciable hydrogen sulfide. Colder (denser) water from the western spring inlet flows into Escobedo without mixing completely and sinks down into the main well where turbulent mixing with deep, warmer water occurs. A lane of dark mineral

precipitate⁵ (probably Mn-bearing) on the spring sediment marks its course. Mixing cold and warm waters then flow upward and in a NNE direction toward the outlet. Because of the large contribution of the low O_2 , warm source, and the short residence time, the entire spring basin is O_2 poor and warm even in the shallows and close to the surface. Vertical profiles of temperature, dissolved oxygen, and light penetration for the main well are presented in Figure 2. The water was clear with spectrally averaged transmittance around $65\% m^{-1}$ in the PAR region.

Primary producers. Unicellular planktonic primary producers were not observed in water sample⁵ nor were conspicuous benthic blooms present on the sediment, even though they were all within the euphotic zone (Fig. 2). Heterogenous stromatolitic assemblages of calcifying cyanobacteria and diatoms, typical of many springs in the region (Winsborough et al. 1994), were present on the shore ledges only. A population of brown, centimeter-sized, gelatinous cyanobacterial

colonies suspended by the upward flow within the bounds of the main well constituted the most conspicuous component of primary producers. Because of their morphology, we refer to them as waterwarts (Fig. 3). We estimate that the population in the well may have been in the tens of thousands of individual waterwarts. A small portion of this population was lying on the steeply sloped sediment of the well, particularly on the southern side. Interestingly, this large population was not always visible during our observational period. During episodes of low water flow from the bottom springs, waterwarts sank to the well bottom and rolled into its cavernous openings, completely disappearing from view until flow resumed again. The episodes of waterwart disappearance we were able to witness lasted on the order of hours to days.

Waterwart structure and composition. Waterwarts were composed of roughly spheroidal to elongated colonies of bacilloid unicellular cyanobacteria embedded in a large amount of gel-like glycan (Fig. 3). According to botanical taxonomy (Komarek and Anagnostidis 1999), they would be assigned to the genus *Aphanothece*. According to bacteriological taxonomy (Castenholz 1989), they would be assigned to the genus *Cyanothece*. However, presently recognized genera of unicellular cyanobacteria do not represent phylogenetically coherent units at the molecular or biochemical level, including *Aphanothece* and *Cyanothece* (Garcia-Pichel et al. 1998). We thus refrain from using taxonomic epithets that might induce unfounded ecological or physiological associations. The cyanobacteria were distributed throughout the colony, although higher population densities occurred at the periphery. The glycan was colorless, and the overall brown appearance of the colonies was due to the cell's phycobilin complement (abundant phycoerythrin). One to several of these colonies, together with smaller budding new colonies, formed a cohesive waterwart. The mean waterwart size (max. diameter) was 0.995 cm ($n = 100$), and the range was $0.4\text{--}1.9\text{ cm}$, but the size distribution was skewed toward larger sizes. The modal size was 0.8 cm . Microscopic observations of DAPI-stained thick sections (1 mm) revealed that the interior of the colonies was completely devoid of bacteria other than cyanobacteria. The waterwarts supported a diverse assemblage of epiphytic microalgae, which included *Phormidium*-like cyanobacteria and diatoms (mostly *Nitzschia* spp.). This assemblage was also found in the internal parts of waterwarts, but only on the contact surface between colonies and not within the glycan of each colony. Mineral crystallites were always observed within waterwarts. Crystals were white to orange and ranged in length from $30\text{ to }200\text{ }\mu\text{m}$. The crystallites were most abundant on the contact surface between colonies, but some mostly larger crystallites were always present within the extracellular glycan of colony interiors (Fig. 3). The surface of the crystallites was free of bacteria, as judged by DAPI staining. Differential centrifugation yielded the following volumetric partitioning: glycan 95.9% , cells 2.8% , and mineral grains 1.3%

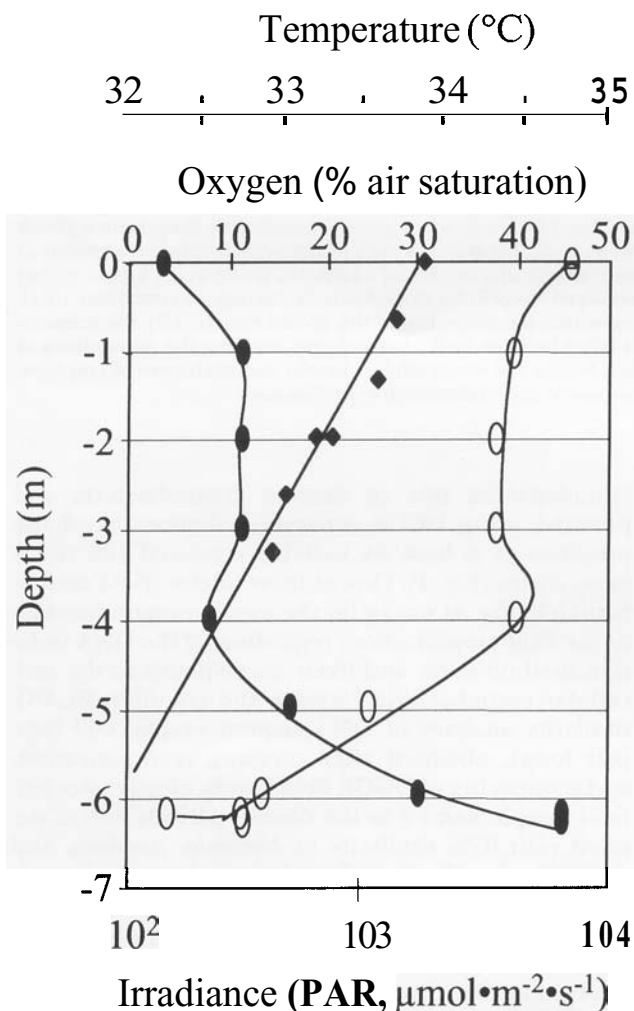


FIG. 2. Vertical profiles of light (\blacklozenge), dissolved oxygen (\circ), and temperature (\bullet) in Escobedo's main well.

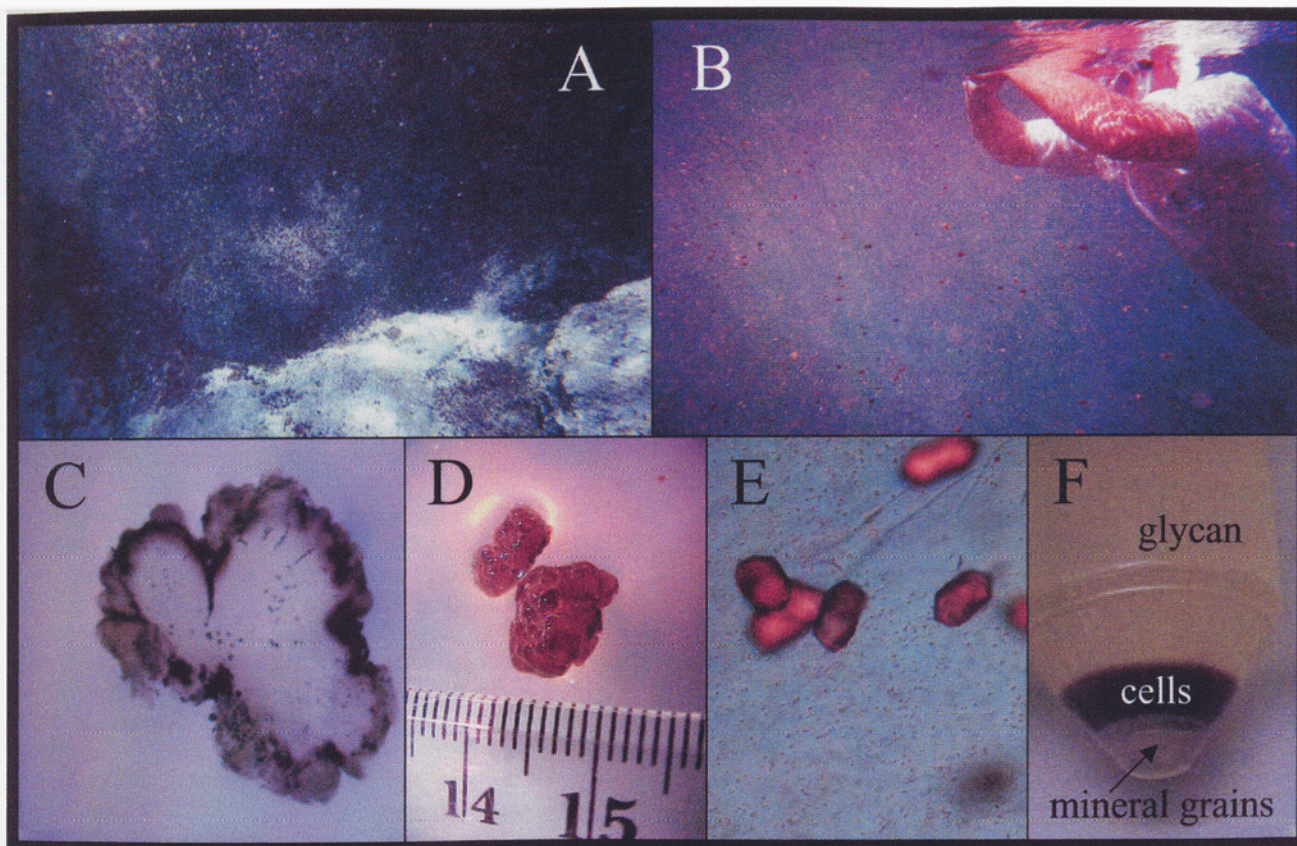


FIG. 3. Aspects of Escobedo's waterwart population and their structure. (A) Underwater view of Escobedo's deep source (from above) with clouds of waterwarts being pushed upward by the jetting waters. (B) Underwater view of the population of waterwarts at shallow depth after disturbance by a swimmer (B. D. W.). (C) Photomicrograph of a sectioned waterwart, made up of lobose glycan colonies. Dark areas close to the surface are accumulations of brown-colored unicellular cyanobacteria. Strings of crystallites (dark dots) can be seen at the contact surface of adjacent colonies and deep within a colony, inside the glycan matrix. (D) Photomicrograph of the external waterwart appearance. (E) Close-up of a contact region between individual colonies showing the populations of unicellular cyanobacteria in the glycan matrix and a group of crystallites. Notice the extracellular sheaths and trichomes of epiphytic cyanobacteria. (F) Glycan, cells, and mineral grains from bulk waterwart slurry after differential centrifugation.

of the total waterwart volume. With respect to their weight composition, waterwarts were 96.2% water (blotted wet weight-to-dry weight ratio) and 3.78% (w/w) solids. The warts had an average buoyant density of $1.034 \pm 0.014 \text{ kg} \cdot \text{L}^{-1}$, significantly lighter than the average buoyant density of typical bacterial cells. Experiments conducted in the laboratory determined that an average minimal upward flow velocity of $0.76 \text{ cm} \cdot \text{s}^{-1}$ was needed to keep waterwarts suspended.

Identity of waterwart microalgal component. Microscopic observation indicated that the bulk of waterwart biomass, responsible for its formation, corresponded to colonial unicellular cyanobacteria. However, attempts to obtain them in culture using various combinations of culture conditions failed repeatedly. Enrichment cultures yielded typically *Phormidium*, *Pseudanabaena*, and *Lyngbya*-like filamentous cyanobacteria, as well as diatoms (*Nitzschia*). All were likely enriched from the epiphytic community. Culture-independent fingerprint analysis of the waterwart community based on PCR amplification of 16S rRNA genes specific for the

cyanobacterial line of descent (cyanobacteria and plastids) using DGGE separation demonstrated the presence of at least six well-differentiated 16S rRNA gene alleles (Fig. 4). One of these alleles (field sample band b in Fig. 4) was by far the most common product in the PCR amplification, regardless of the DNA isolation method used, and likely corresponds to the unicellular cyanobacteria forming the colonies. BLAST similarity analyses of DNA sequences (ca. 600 base pair long), obtained after excision, reamplification, and sequencing of DGGE field bands, clearly associate field sample band a to the diatom plastids line of descent with 97% similarity to *Navicula*, *Amphora*, and *Odontella* plastids. BLAST analysis of the main band b did not find very close matches, yielding a group of unicellular cyanobacteria (*Merismopedia glauca*, *Cyanothece* PCC 7424, and *Cyanothece* ATCC 51142) as the closest matches, but only with 89% sequence similarity. Additionally, this sequence was 93% similar to various *Microcystis* isolates, albeit only 400 base pair could be compared in this case. No clear matches were

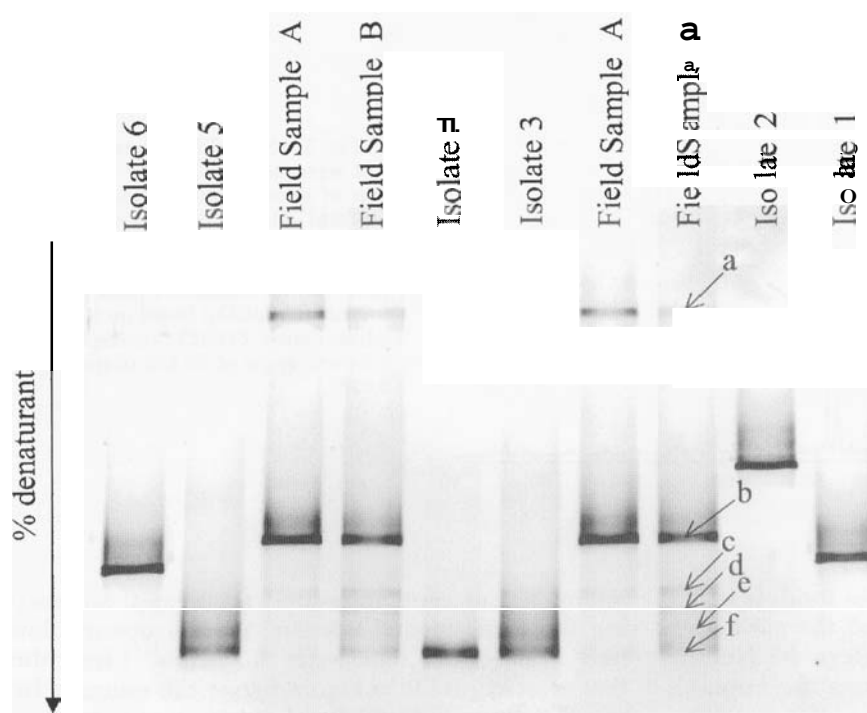


FIG 4 Denaturing gradient gel electrophoretic separation (DGGE fingerprint) of 16S rRNA gene fragments PCR amplified specifically from oxygenic phototrophs (cyanobacteria and plastids). Amplified fragments have equal length, but each band represents a 16S rRNA gene allele of unique melting characteristics (sequence). Isolated DNA from field samples of waterwarts, or isolated DNA from unialgal, clonal isolates from enrichment cultures of waterwarts were used as template for separate PCR amplification and the products loaded in each lane (as labeled). In the case of field samples, two different DNA isolation methods were used (A and B), and each was loaded in two separate lanes for ease of comparison. Specific bands are labeled for discussion (see text).

found for the remaining field bands (c, d, e, and f). Band c had 90%–91% sequence similarity to various strains of *Spirulina*, *Lyngbya*, and *Phormidium*. Sequences from bands c, d, and f were very similar among themselves (>99%), and all gave a strain of *Phormidium autumnale* as the closest cultivated match, but again with only 90% similarity. With respect to the identity of the isolates enriched from waterwarts, several observations are interesting to note. Isolates 1 and 6, morphologically a thin 1.5 μm wide green *Phormidium*, had indistinguishable DGGE band positions between them, but this band position was not represented in the field sample fingerprints, indicating that they were not among the dominant epiphytes. The same holds true for isolate 2, a 2–3 μm wide *Pseudanabaena*. Isolate 4, morphologically, an 8–10 μm wide *Lyngbya*, matched the position of field band f, but it is yet unclear if this implies also sequence similarity. Isolates 3 and 5 were brown, phycoerythrin-containing, 3–5 μm wide filamentous forms, morphologically assignable to *Phormidium*. The DGGE fingerprints of isolates 3 and 5 are quite intriguing because they seem to contain at least four divergent 16S rRNA gene alleles and coincide with field bands c–f.

Identity of mineral precipitate. The mineral precipitate found within the colonies was determined to be calcite using a combination of optical microscopy and x-ray diffraction analyses. Optically, the crystallites showed a bladed internal fabric, suggesting that they are in fact crystal aggregates rather than single crystals. X-ray diffraction results revealed that although the mineral fraction belonged to the calcite family, there was a consistent displacement of d-spacing of

the primary diffraction peak from an expected value of 3.030 Angstroms (pure calcite) to an observed value of 3.028 Angstroms (Fig. 5). This is suggestive of some type of limited cation substitution. Electron microprobe analysis of individual mineral grains (Table 1) revealed that the crystallites consist of low magnesium calcite, with an average Mg content of 1.76% by weight and with no measurable iron. Strontium averaged 1.74% by weight. Surprisingly, sulfur averaged 2.03% by weight.

DISCUSSION

Natural selection by the hydrological regime. Escobedo's water residence time (11 min) is significantly shorter than the fastest doubling times measured in any microorganism. This is the likely reason that no typical planktonic populations exist there. To maintain a stable population, attachment to resist flow, or movement to oppose it, is necessary. The lack of benthic populations may be due to efficient grazing on the soft sediment by local fish populations. Sinking by gravity may provide the necessary opposing force to the upward flow of water within the main well. A vertical profile of space-averaged upward flow velocity within the central well was calculated from total spring discharge and well cross-sectional area as a function of depth (Fig. 6). According to these calculations, minimal sinking or downward swimming speeds between 1.2 and 0.5 $\text{cm}\cdot\text{s}^{-1}$ are needed to keep a population deeper than 1 m, thus avoiding lateral flow and outwash. Maximal swimming speeds for unicellular prokaryotes and eukaryotes (ca. 0.6 and 1 $\text{mm}\cdot\text{s}^{-1}$, respectively, Garcia-Pichel 1989) are too slow by one order of magnitude to counteract such flow rate. The

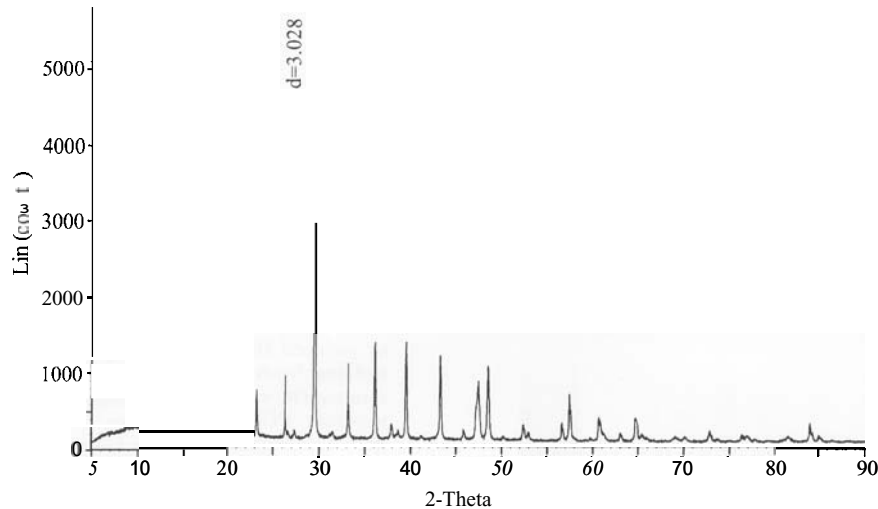


FIG. 5. X-ray diffractogram for mineral separates obtained by centrifugation of disaggregated waterwarts. Major and minor peak positions are indicative of calcite with small but consistent shift from expected values for pure calcite. Dominant peak position for calcite (CaCO_3) based on ICDD database (entry 240027) corresponds to a 2-theta angle of 29.453 (d -spacing = 3.028).

sinking of roughly spherical particles in fluids is well described by Stokes Law, provided that the particles sink in an environment of low (<1) Reynolds Number. The Reynolds Number (N_R) gauges the importance of viscous versus inertial forces that oppose movement within a fluid. Stokes Law states that particles will sink with a constant, terminal velocity, V , equal to $2 g R^2 (\rho - \rho_o) (9 \eta)^{-1}$, where ρ is the density of the particle and g is the acceleration of gravity. Terminal sinking velocities, with $N_R \ll 1$, of $0.22 \mu\text{m}\cdot\text{s}^{-1}$ (or $2.17 \times 10^{-5} \text{cm}\cdot\text{s}^{-1}$) can be calculated for typical $1 \mu\text{m}$ wide bacterial cells ($1.08 \text{kg}\cdot\text{L}^{-1}$, Guerrero et al. 1985). Because this velocity is much smaller than the average upward flux velocity $0.5\text{--}1 \text{m}$ deep in the well, typical bacteria would be easily swept away. Solving Stokes equation to match the flow velocity at 1m depth ($0.56 \text{cm}\cdot\text{s}^{-1}$, and using $\eta = 0.007 \text{g}\cdot\text{cm}\cdot\text{s}^{-1}$ and $\rho_o = 0.997 \text{g}\cdot\text{cm}^{-3}$, typical for freshwater at 30°C), we determine that to maintain single microbial cells within the well, they should be at least 3mm in diameter. In fact, this situation is no longer appropriately described by Stokes Law, because the corresponding N_R is larger than one and inertial forces become important. It is clear that the hydrological regime present in Escobedo during active flow periods will tend to wash out plankters of small size and select for

millimeter- to centimeter-sized aggregates. Subtracting the experimental value of average upward flow needed to levitate waterwarts ($0.76 \text{cm}\cdot\text{s}^{-1}$) from the flow velocity profile in Figure 6, one can estimate the actual average net speed and direction of waterwarts at different depths within the well (indicated as velocity vectors in Fig. 6). According to this model, water-

TABLE 1. Elemental composition for mineral grains extracted from Escobedo's waterwarts according to electron microprobe analysis.

Element	Average content (wt %)	Standard deviation (range)	Number of analyses
Mg	1.76	0.69 (0–2.71)	28
Fe	b. d. l. ^a		28
S	2.84	0.84 (0.05–2.68)	25 ^b
Sr	1.74	2.45 (0–12.7)	28

^a b. d. l., below detection limit. Minimum detection limit for Fe was 0.053, for Mg 0.079, for S 0.098, and for Sr 0.026.

^b Three analyses were run before the addition of a sulfur standard.

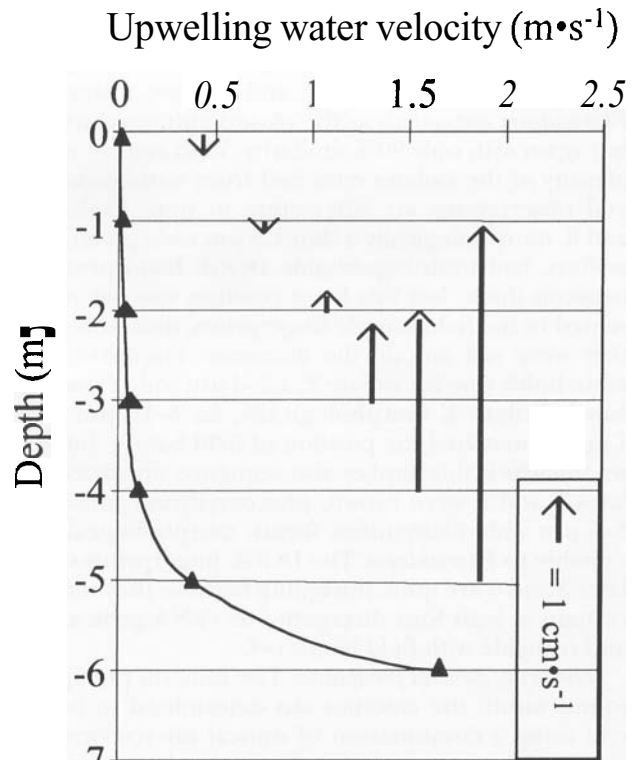


FIG. 6. Vertical profile of the space-average upwelling water velocity in Escobedo's main well. Flows have been calculated from well cross-sectional area and spring outflow. Drawn at each depth is the calculated average vertical velocity vector for waterwarts as a function of local flow and sinking speed.

warts are pushed upward rapidly at depth, slowing down as they reach the average depth of zero velocity (approx. 1.35 m). Above that depth they sink back into the well. This simple model explains the continued presence of the waterwart population in the well, with the single imposed parametric value of appropriate levitation velocity. The factors affecting such velocity, under obvious biological control, are discussed in the following section.

Mineral and biological ballast within waterwarts. Given the measured buoyant density ($1.034 \text{ kg}\cdot\text{L}^{-1}$) of waterwarts and their volumetric partitioning into glycan, cellular, and mineral fractions, some relevant calculations are possible. First, it can be calculated that with typical bacterial buoyant cell densities of $1.08 \text{ kg}\cdot\text{L}^{-1}$ and a typical density for calcite of $2.75 \text{ kg}\cdot\text{L}^{-1}$, cells contribute $0.030 \text{ kg}\cdot\text{L}^{-1}$ to the buoyant density of waterwarts, whereas calcite concretions contribute $0.035 \text{ kg}\cdot\text{L}^{-1}$. The rest, $0.968 \text{ kg}\cdot\text{L}^{-1}$, is contributed by the hydrated glycan. The buoyant density of the glycan fraction must be ca. $1.010 \text{ kg}\cdot\text{L}^{-1}$, very close to the density of water at 30°C . Thus, striving to increase size by accumulating large amounts of extracellular glycan will be at the expense of a loss in buoyant density of the colony and partly defeat the purpose of increasing sinking velocity. Without the mineral fraction (maintaining cells and glycan in the same volumetric ratios as determined) the waterwart's density should be $1.012 \text{ kg}\cdot\text{L}^{-1}$. Thus, the mineral fraction, although small, makes a significant contribution to the waterwart's ballast and allows it to sink at a speed sufficient to remain within the bounds of Escobedo's main well.

Extracellular control of mineral ballast. Whereas most algae in the region are calcifying and stromatolitic (Winsborough and Golubic 1987, Winsborough et al. 1994), including other algal communities in Escobedo's spring, waterwarts apparently control this process. Under a purely thermodynamical view, the waterwart's main constraint in controlling extracellular mineral ballast is not so much how to promote its formation but rather how to avoid its generalized occurrence. In macroscopic assemblages of photosynthetic organisms (such as benthic biofilms or large colonies), diffusion limitation of mass transport promotes localized photosynthesis-driven increases in environmental pH. This in turn raises the carbonate ion concentration, further increasing the calcite supersaturation factors in the immediate vicinity of the cells (de Vrind-de Jong and de Vrind 1997). To avoid generalized calcite precipitation in the waterwarts, the initial nucleation process must be prevented. It is known that polymeric substances can act to modify the nucleation energy for calcite (Manoli et al. 1997, Hosoda and Kato 2001). Both promotion and prevention effects can be found in the chemically diverse extracellular polymers of cyanobacteria. Pentecost and Bauld (1988) demonstrated that extracellular glycan sheaths of some *Lyngbya* and *Scytonema* promote nucleation, but not those of *Entophysalis* and *Pseudanabaena*. We suggest that the chemical composition of the water-

wart's glycan could be such that initial steps of calcite nucleation are prevented at most sites and yet promoted or allowed at particular sites, so that enough ballast is attained. The preferred distribution of calcite in the interfaces between individual colonies and the orderly arrangement of microcrystalline aggregates implies such a controlled mechanism, but direct evidence for this hypothesis must be sought in chemical analyses of purified glycan. Interestingly, the fact that much of the calcite is found at the interfaces between colonies, in close proximity to the epiphytic microalgae, suggests the epiphytes may control ballast precipitation. If this were corroborated, it would indicate that the coordinated action of the community as a whole, not just the unicellular cyanobacteria forming the colonies themselves, is needed to achieve hydrodynamically stable waterwarts.

Strontium substitution in calcite. Further analyses of the calcite ballast is warranted given the consistent displacement of d-spacing of the primary x-ray diffraction peak and the percent averages by weight of Sr and S in the calcite. Cyanobacteria have been involved with the nucleation of strontium calcite elsewhere (Ferris et al. 1995). The effect of Sr substitution on lattice structure and crystal form and the coordination site for sulfur are still under investigation. Of special interest in this regard is the precise biogeochemical process that controls carbonate precipitation, the role of the glycan matrix in crystal nucleation, and the potential for mineralogical biosignatures specific to this environment.

CONCLUSIONS

The particular hydrological conditions created in Escobedo's spring after digging the central well during the 1960s likely set the stage for the selection of a unique form of jet-suspended, calcite-ballasted, colonial cyanobacterial community with simple but apparently sufficient adaptations to the local environment. In the case of Escobedo's spring "buoyostat," the selective rules are simple: too heavy and waterwarts sink and are eventually buried in the soft turbated sediment, or too light and they will be washed out downstream. Only within the physical bounds allowed by the hydrodynamic regime, their fitness coefficient is 1; otherwise, it is 0. In our view, the combination of macroscopic colony formation and controlled calcite precipitation represent a simple solution to the problem, because both traits are common among cyanobacteria. We are not aware of the presence of suspended waterwarts in other springs in the area or elsewhere. Morphologically similar (macroscopic *Aphanothece*-like) colony-forming cyanobacteria are known from benthic environments, but they only rarely and temporarily become planktonic (Komarek and Anagnostidis 1999). It is interesting to speculate that Escobedo's waterwarts may have originated from benthic colonial forms already adapted to life on soft spring sediment, similar to those described for *Nostoc pruni-forme* (Dodds and Castenholz 1987).

Note added after review. During the fall of 2001, Escobedo's outlet was dammed in an intended restoration effort. On a visit in January 2002, water level had risen by 2–3 m and the hydrological characteristics changed drastically. We found evidence for a large mortality event in the waterwart population, with large numbers of chlorotic colonies buried in the sediment, but a small number of apparently healthy waterwarts were still present close to the bottom source. Apparently similar colonies made up of *Aphanothece*-like cyanobacteria were also found in a shallow bottom-fed pool floating on the surface of a highly hydrated fluid sediment.

We thank the Mexican environmental agency, SEMARNAT, for permission to sample and conduct research in the Cuatro Ciénegas Biosphere Reserve and Mr. Arturo Contreras for field guidance. This paper is dedicated to the memory of Dr. Wendell "Minck" Minckley, long-time conservation advocate of the Cuatro Ciénegas treasures, who introduced us to the area. This research was funded by the NASA Astrobiology Institute (grant NCC2-1051).

- Castenholz, R. W. 1989. Oxygenic photosynthetic bacteria. In Staley, J. T., Bryant, M. P., Pfennig, N. & Holt, J. G. [Eds.] *Bergey's Manual of Systematic Bacteriology*. Williams & Wilkins, Baltimore, Vol. 3, pp. 1710–28.
- Camacho, A., Garcia-Pichel, F., Vicente, E. & Castenholz, R. W. 1996. Adaptation to sulfide and to the underwater light field in three cyanobacterial isolates from Lake Arcas (Spain). *FEMS Microbiol. Ecol.* 21:293–301.
- de Vrind-deJong, E. W. & de Vrind, J. P. M. 1997. Algal deposition of carbonates and silicates. In Banfield, J. F. & Nealson, K. H. [Eds.] *Geomicrobiology: Interactions Between Microbes and Minerals*. Mineralogical Society of America, Washington, DC, pp. 267–73.
- Dodds, W. K. & Castenholz, R. W. 1987. Effects of grazing and light on the growth of *Nostoc pruniforme* (Cyanobacteria). *Br. Phycol. J.* 23:219–27.
- Ferris, F. G., Frattton, C. M., Gertis, J. P., Schultzelam, S. & Lollar, B. S. 1995. Microbial precipitation of a strontium calcite phase at a groundwater discharge zone near Rock Creek, British Columbia, Canada. *Geomicrobiol. J.* 13:56–67.
- Garcia-Pichel, F. 1989. Rapid bacterial swimming measured in swarming cells of *Thiovulum majus*. *J. Bacteriol.* 171:3560–3.
- Garcia-Pichel, F., Nübel, U. & Muyzer, G. 1998. The phylogeny of unicellular, extremely halotolerant cyanobacteria. *Arch. Microbiol.* 169:469–82.
- Grall, G. 1995. Cuatro Ciénegas: Mexico's desert aquarium. *Natl. Geogr.* 188:85–97.
- Guerrero, R., Pedrós-Alió, C., Schmidt, T. M. & Mas, J. 1985. A survey of buoyant density of microorganisms in pure cultures and natural samples. *Microbiologia* 1:53–65.
- Hosoda, N. & Kato, T. 2001. Thin film formation of calcium carbonate crystals; effects of functional groups of matrix polymers. *Chem. Mater.* 13:688–93.
- Komarek, J. & Anagnostidis, K. 1999. *Cyanoprokaryota. I. Teil. Chroococcales. Süßwasserflora von Mitteleuropa*. Gustav Fischer Verlag, Heidelberg, Germany, 548 pp.
- Konopka, A. 1989. Metalimnetic cyanobacteria in hard-water lakes: buoyancy regulation and physiological state. *Limnol. Oceanogr.* 34:1174–84.
- Manoli, F., Koutsopoulos, S. & Dalas, E. 1997. Crystallization of calcite on chitin. *J. Crystal Growth* 182:116–24.
- Nübel, U., Garcia-Pichel, F. & Muyzer, G. 1997. PCR primers to amplify 16S rRNA genes from cyanobacteria. *Appl. Environ. Microbiol.* 63:3327–32.
- Pentecost, A. & Bauld, J. 1988. Nucleation of calcite on the sheaths of cyanobacteria using a simple diffusion cell. *Geomicrobiol. J.* 6:129–36.
- Pentecost, A. & Whitton, B. A. 2000. Limestones. In Whitton, B. A. & Potts, M. [Eds.] *The Ecology of Cyanobacteria*. Kluwer Academic Publishers, Dordrecht, pp. 257–79.
- Walsby, A. 1994. Gas vesicles. *Microbiol. Rev.* 58:94–144.
- Winsborough, B. M., Seeler, J.-S., Golubic, S., Folk, R. L. & Maguire, B. Jr. 1994. Recent fresh-water lacustrine stromatolites, stromatolitic mats and oncoids from Northeastern Mexico. In Bertrand-Sarfati, J. & Monty, C. [Eds.] *Phanerozoic Stromatolites II*. Kluwer Academic Publishers, Dordrecht, pp. 71–100.
- Winsborough, B. M. & Golubic, S. 1987. The role of diatoms in stromatolite growth: two examples from modern fresh-water settings. *J. Phycol.* 23:194–201.